IOP Conf. Series: Materials Science and Engineering **8** (2010) 012035 doi:10.1088/1757-899X/8/1/012035

The effects of switching time and $SrTiO_{3-x}N_y$ nanostructures on the operation of $Al/SrTiO_{3-x}N_y/Al$ memristors

Andrey Shkabko[1*], Myriam H Aguirre[1], Paul Hug[1], Anke Weidenkaff[1], Ivan Marozau[2] and Thomas Lippert[2]
[1]Empa, Solid State Chemistry and Catalysis, Ueberlandstrasse 129, 8600 Duebendorf, Switzerland
[2]Paul Scherrer Institut, 5232 Villigen PSI, Switzerland
E-mail: andrey.shkabko@empa.ch

Abstract. The nanostructure and switching properties of the $Al/SrTiO_{3-x}N_y/Al$ memristors have been investigated. It was found that the formation of stacking faults defects in the perovskite structure during plasma nitridation facilitates resistivity switching in $Al/SrTiO_{3-x}N_y/Al$ memristors. From thermal emission measurements we observed local heating of the $Al/SrTiO_{3-x}$Ny anode interface (285ºC) during switching when the interface becomes rectified due to the formation of locally undoped region. A model for resistivity switching and parameters affecting the memristor operation is discussed considering the electromigration theory. The I-V curves are analyzed taking into account the tunnel barrier formations and an inhomogeneous Schottky barrier modification at the anode interface.

1. Introduction

Memristors attract the attention of scientists for more than 40 years [1, 2]. This device is defined as two terminals in which the magnetic flux, Φ, between two points is a function of the electric charge, q(t), passing through the device. It is characterized by the memristance $M(q,t) = d\Phi / dq = V(t) / I(t)$, where V(t) and I(t) – is the time dependent voltage and current, respectively. The memristance function $M(q,t)$ is the analog to the resistance and a simple consequence of the theory is $M(q,t) =$ constant, revealing the ohmic behavior. If $M(q,t) \neq$ const, the memristance is a non-trivial function of charge and time.

A memristor can be used for memory applications and is characterized by resistance states, which are stable in time. The resistance states can be read out by low voltages (small charge transport), which do not change the resistance states. However, if the electronic current density becomes too high, the resistance switches. One possible mechanism of resistance switching is ion and/or vacancy migration on the nanometer scale in close vicinity to interfaces [3, 4]. This kind of ion migration is closely related to electromigration studies, where failure analysis of metal contacts (Al, Cu, Au, Pt, Ir) upon decrease of size and increase of current densities [5-7] were performed. In these studies, the processes of the electromigration is current-induced, thermally assisted, and strongly dependent on the ionic diffusion constants, the electrical resistivity of materials, structure and stress of the materials [8].

* To whom any correspondence should be addressed.

In this paper we summarize the parameters which affect the memristance in Al/$SrTiO_{3-x}N_y$/Al in order to define a possible improvement of the memristor performance.

2. Experimental

Commercially available $SrTiO_3$ (100) single crystals (Crystec) grown by the Verneuil method were microwave plasma treated in a quartz tube with 125 ml/min ammonia flow as described elsewhere [9]. The samples were mechanically polished using diamond paper with a grain size of 0.5 µm in order to avoid any other possible non-perovskite-type contaminations from the topmost surface. The average composition of the samples surface was $Sr_{0.92}TiO_{2.44}N_{0.40}$, as evaluated by XPS. The chemical stability of the $SrTiO_{3-x}N_y$ samples were examined by thermogravimetric analysis (TGA) in synthetic air (80% N_2, 20% O_2) using a NETZSCH STA 409CD thermobalance coupled with a 409C Aeolos Quadrupole Mass Spectrometer (MS) by a heated quartz capillary with 20^0Cmin^{-1} heating rate. TEM analysis of the interfaces was performed in a Philips CM30 microscope. For the resistivity switching measurements, the contacts made of 25µm Al wire and separated by 0.25 mm were bonded on the surface by an ultrasound wirebonder (Delvotek 4250). The current-voltage (I-V) curves were measured by a 2 point method [10] using a Keithley 2602 DC current source operated at constant voltage mode with steps of 100µV/s. The electrical resistance failure analysis was performed by a Hamamatsu Phemos-1000 IR-confocal emission microscope using optical laser beam excitation (1.3 µm) induced resistance change (OBIRCH).

3. Results and discussions

The TGA results reveal a thermal stability of the samples up to 350 ^0C. At higher temperatures (>350 ^0C) the back reaction of the oxynitride to the oxide occurs [11]. The samples take up oxygen and release nitrogen resulting in a final composition of stoichiometric $SrTiO_3$, as confirmed by XPS.

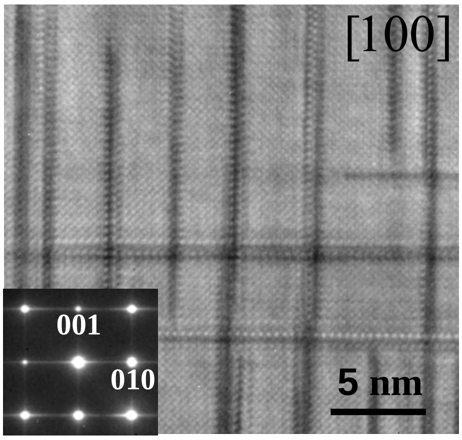

Figure 1. HRTEM of $SrTiO_{3-x}N_y$ in [100] zone axis with electron diffraction pattern inset.

Figure 1 presents the HRTEM micrograph of the [100] zone axis of $SrTiO_{3-x}N_y$. It shows defects parallel and perpendicular to the surface of the sample. The electron diffraction pattern, inset figure 1, corroborates the existence of defects showing diffuse intensity or streaking along the <001> and <010> directions. The diffuse scattering in the marked directions appears when faults in the stacking sequence of the atomic planes exist. An important feature of the defect nanostructure is the facilitation of electroformation and resistivity switching compared to samples without defects [9]. $SrTiO_{3-x}N_y$ prepared with defects, as a conducting channels, does not require a long/hard electroformation process prior to the first reliable switching [9, 12, 13]. The appearance of the planar defects and their instability at particular I-V conditions can be explained the electromigration theory and the existence of the so called Blech length [14]. According to this theory, conducting samples of shorter Blech length withstand higher current densities in order to start ion migration. For our particular case, assuming that the electron conduction presumably occurs through defects (see for example Fe-doped $SrTiO_3$ [15]), samples with stacking faults do not sustain the current and facilitate reversible migration. In the opposite case, samples with small density of defects, or short length defects will be stable for similar currents.

It has been shown that $SrTiO_{3-x}N_y$ exhibits a metallic like conductivity and a comparatively low resistance (less than 1 Ohm) [16], while the interface resistances between metal contact/$SrTiO_{3-x}N_y$ are two orders of magnitude higher (100 Ohm) which suggests a possible formation of Schottky barriers at the interfaces. In order to study these interfaces prior to electroforming, Al/$SrTiO_{3-x}N_y$/Al was examined by the OBIRCH methods using low current densities which do not change the linear I-V characteristics obtained by 2 point measurements.

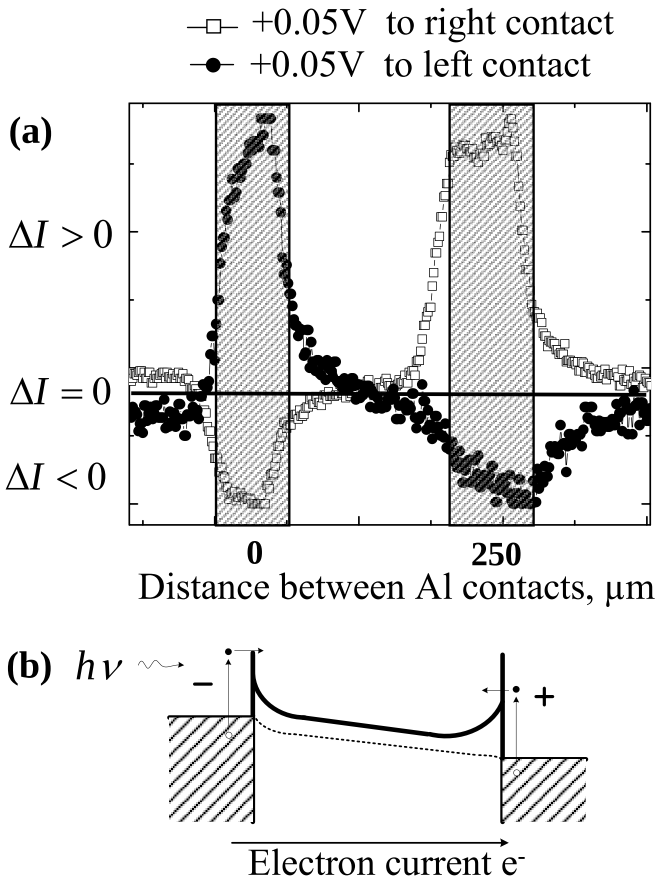

Figure 2. (a) Current signal (OBIRCH) as a function of distance between Al electrodes, (b) Energy-band diagram for back-to-back Schottky device during application of +0.05V to the right electrode and photoexcitation processes induced by laser.

The OBIRCH method uses simultaneously two processes: a fast laser beam excitation of the lateral surface of the $SrTiO_{3-x}N_y$ area, and the detection of the resistance changes at a fixed voltage: $\Delta I \approx -I^2 \Delta R / V$ [17]. In figure 2a the line profiles of the current change (resistance change) are presented as a function of the distance between the Al contacts with two fixed voltage polarities (+0.05V applied to the right contact and -0.05V applied to the left contact). The observed current changes are similar to those described for Al/n-type Si/Al back-to-back Schottky junctions [17]. Photoexcitated electrons move from the n-doped $SrTiO_{3-x}N_y$ to the Al electrodes [18]. The total current change, $\Delta I > 0$, which is the sum of the electrical and photoexcitation currents, is induced at the negatively biased electrode while $\Delta I < 0$ is induced at the positively biased electrode (see figure 2b). The reversal of the polarity [(+) left electrode, (-) right electrode], induces a current change, i.e

$\Delta I > 0$ at the negatively biased right electrode and $\Delta I < 0$ at positively biased left electrode. Summarizing, the positively biased electrode always shows high resistance (high current change) at low I-V conditions similar to Schottky barriers. Thereby, as prepared Al/$SrTiO_{3-x}N_y$/Al can therefore be considered to be equivalent to back-to-back Schottky diodes.

It is noteworthy that the Schottky barrier at these interfaces consists of inhomogeneous Schottky barriers profiles which is due to the presence of stacking faults defects and a nearly defect-free perovskite structure at the surface of $SrTiO_{3-x}N_y$ [19, 20]. The currents flow through individual patches represented as defects and defect-free regions of various sizes. However, the conductivities and Schottky barrier heights at the stacking fault defects as well as their concentrations and distributions requires further studies in order to apply a model (for example Tung's model [19]) to describe the electric current through the metal-semiconductor interfaces.

Memristance, according to Ref. [3], can be described by $M(q) = R_{HRS}(1 - \mu_V R_{LRS} q(t) / D^2)$, where R_{HRS}, R_{LRS} – are the resistance values in the high resistance (HRS) and low resistance states (LRS), respectively, while μ_V is the ion mobility, *q(t)* is the electrical charge passing through the memristor, and D is the size of the memristor [3]. We would like to emphasize, that in a memristor the changes of the resistance states (LRS, HRS) are localized at the anode interface [9]. High voltages (in our case more than 3V) induce thermal heating by electron current. The local temperature of the anode during the switching process increases to 285^{0}C, as detected by the IR camera. An increase of the temperature will, according to the memristance function, increase the ion mobility and hence the thickness of the undoped region of the sample, $w(t) = \mu_V R_{LRS} q(t) / D$. In the case of ion migration not only the temperature of the environment plays a crucial role during switching, but also the current-induced temperature. A large density of electron current intrinsically heats the anode interface thereby enforcing electromigration [6]. Nevertheless, the highest measured temperature of 285 ^{0}C is lower than the thermo-chemical stability limit of ~350 ^{0}C for $SrTiO_{3-x}N_y$ as it was measured by TGA.

To relate the maximum temperature of the memristor switching with the oxidation of $SrTiO_{3-x}N_y$, a method with a higher sensitivity for the N/O content must be used. We performed four probe measurements in air atmosphere at low voltages while the temperature was increased. During the first heating cycle to 200 ^{0}C, the metallic-like conductivity reveals a steep increase of the resistance. A further increase of the temperature (220^{0}C, 320^{0}C, and 450^{0}C) gradually oxidizes the sample surface which results in an increase of the total resistance and a metal-to-semiconductor transition, in figure 3. An additional thermal oxidation of the anode during the resistance switching and intrinsic heating to 285^{0}C can therefore not be excluded, since all experiments were performed in air.

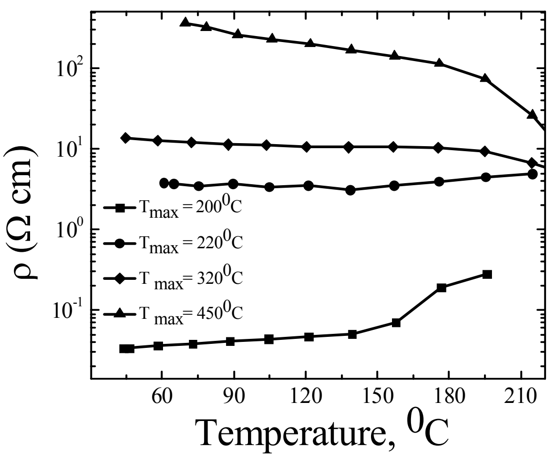

Figure 3. Four point resistance measurements of $SrTiO_{3-x}N_y$ for an increase of the temperature to 200^{0}C, 220^{0}C, 320^{0}C and 450 ^{0}C.

An intrinsic electron heating increases not only the anion electromigration by orders of magnitude [13] but also surface oxidation which could result in a decrease of the memristor reliability in air. In order to test the endurance, write-erase voltage pulses were applied.

The 100μs long pulses of ± 4V are followed by read-out voltages of 0.1V which do not change the stabilities of the HRS and LRS (inset figure 4a). The R_{HRS}/R_{LRS} ratio decreases from 10 to 5 after 10^3-10^4 cycles, as shown in figure 4a. The long-term stability of these states was tested first by 5μs long read-out pulses on the initial LRS and in a second measurement on the HRS (see figure 4b). A negligible degradation of these states after 10^5 sec shows good retention properties of the memristor. However, if we perform experiments in vacuum or in an inert atmosphere a thermal oxidation of the memristor will be prevented and its retention and endurance properties will be improved, since the additional oxidation of the memristor degrades the switching properties [21].

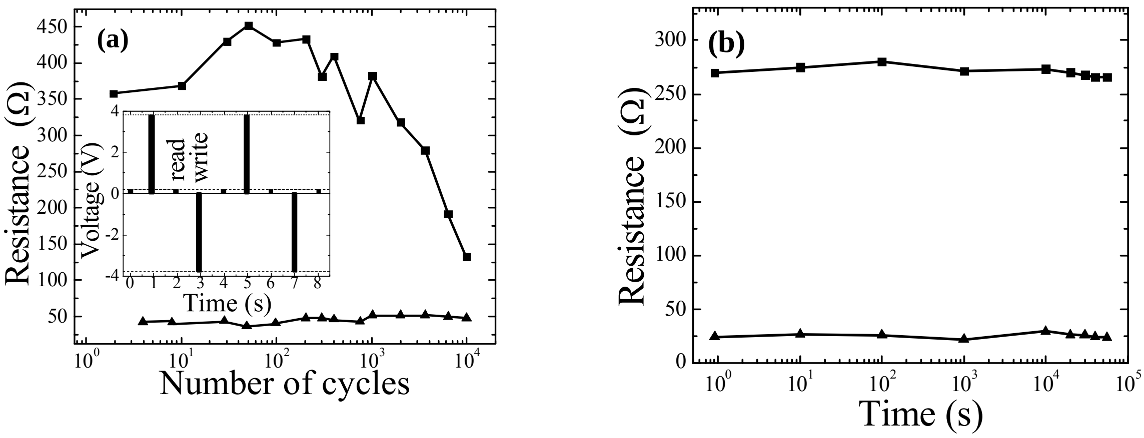

Figure 4. (a) Write-erase endurance tests of a Al/$SrTiO_{3-x}N_y$/Al memristor. The inset shows the sequence of read-write-erase cycles, (b) Stability of the resistance in the LRS and HRS states.

The memristor operation is a complex process involving both ion and electron conductivity and it is still challenging to describe the entire I-V characteristics theoretically. Nevertheless, it is possible to describe the low voltage range of the I-V curve assuming that the current-induced electromigration process at high voltages is completed (or has not yet started). The electric charge carriers, in our case electrons, move through the stable crystal defect nanostructure as displayed in figure 5. The as-prepared Al/$SrTiO_{3-x}N_y$/Al shows linear I-V curves representing the LRS. In this case the anode interface represented by an Al contact which is bonded to the surface of $SrTiO_{3-x}N_y$. The gray pattern shown in the in the scheme view of the $SrTiO_{3-x}N_y$ sample (figure 5) represent stacking fault defects which serve as preferential channels for the electronic and ionic transport [9, 15].

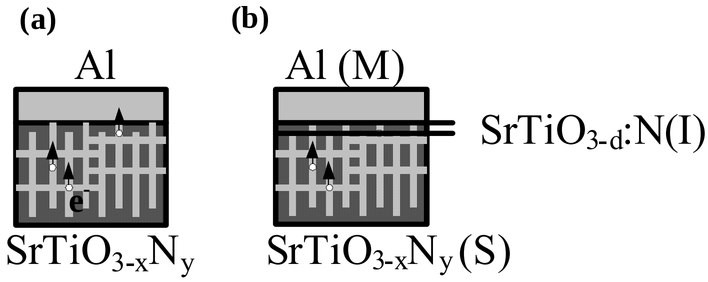

Figure 5. Scheme of the anode interfaces in (a) LRS and (b) HRS. Defects like stacking faults or dislocations are represented by stripes.

Both anode and cathode representations are equal (the cathode is not shown) and the Schottky barrier heights at the interfaces are small (i.e. nearly ohmic contacts) due to the high doping level of $SrTiO_{3-x}N_y$ [16].

If high voltages (>+3V) are applied to the anode, oxygen/nitrogen migrate to the anode interface along the stacking fault defects to form a highly resistive $SrTiO_{3-\delta}$:N layer with variable thickness (HRS), as shown in figure 5b. In the HRS the thickness of the undoped layer at the anode interface increases with time [3, 22] due to a higher amount of anions migrating to the anode. This results in a decreasing R_{HRS} with time, as shown in figure 6.

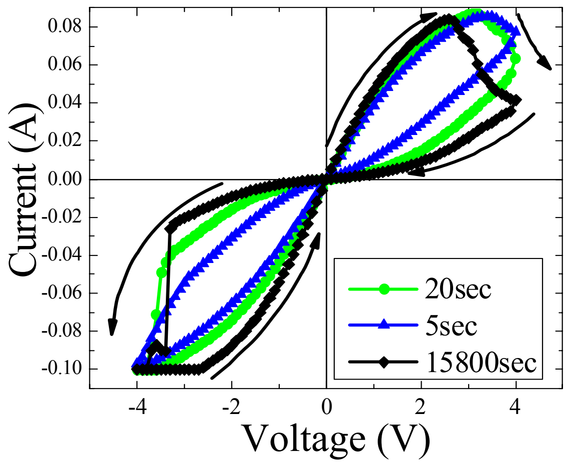

Figure 6. I-V curves for increasing time per loop (5s to 15800s) measured for the same maximum applied voltage of 4V.

A further increase of the voltage to +4.2V increases the R_{HRS} as compared to +3V, which is shown in the inset of figure 7 [9]. Having an overall small Schottky barrier height at the cathode interface, where changes of the resistances are negligible, the Al/$SrTiO_{3-x}N_y$/Al memristor can be considered as a metal-insulator-semiconductor (MIS) capacitor [18], where M is the Al anode, I is the non-conducting $SrTiO_{3-\delta}$:N layer, and S is the $SrTiO_{3-x}N_y$ layer (see figure 5b). It is known for MIS junctions, that different tunneling mechanisms such as Fowler-Nordheim tunneling, direct tunneling, etc., can occur, depending on the thickness of the oxide layer [18]. This suggests different mechanisms of electronic conductivity through the tunnel barrier in the HRS and the ability to perform as a multibit memory due to the different R_{HRS} values.

In addition, inhomogeneous Schottky barriers have also to be taken into account due to local variations of the barrier potential caused by mobile anions. Both models are based on a thermionic emission model. The forward current consists of thermionic emission current multiplied by additional terms which for simplicity will be neglected. The standard thermionic-emission equation for Schottky barriers at the anode interface, i.e. when the electronic current flows in forward direction, can be expressed as: $\phi_{b1} = (kT/q)[A^{**}T^2/J_0]$, where $A^{**} = 156$ A/cm^2-K – is the Richardson constant for $SrTiO_3$ [23], J_0 - is the saturation current as extrapolated from the current density at zero voltage, k – is the Boltzmann constant, q – the electron charge and T – the absolute temperature of the anode. The estimated values of the Schottky barrier height increase with applied voltage, reaching ϕ_{b1}~0.48 eV after applying +4.2V, as displayed in figure 7. This is in good agreement with calculated and theoretically predicted values for the Schottky barrier height of ~ 0.53eV in Al/$SrTiO_3$ junctions [24].

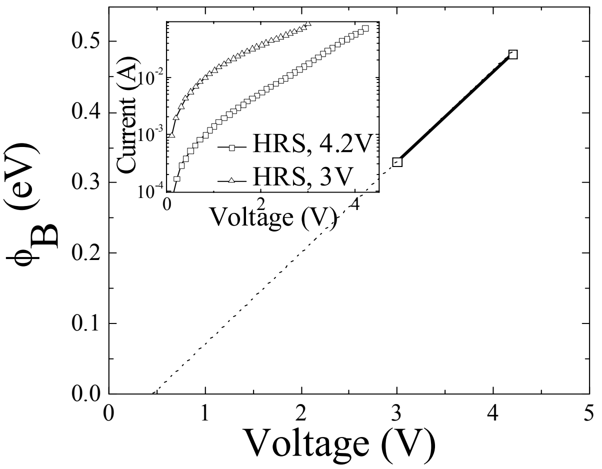

Figure 7. Calculated Schottky barrier height in the HRS after application of +3V and +4.2V. The inset shows forward current characteristics for the HRS of the Al/$SrTiO_{3-x}N_y$/Al memristor, the dotted line is included to guide the eye.

4. Conclusions

We have shown that in Al/$SrTiO_{3-x}N_y$/Al structures the process of electromigration is current-induced and thermally assisted at the $SrTiO_{3-x}N_y$ surface of the anode interface where stacking fault defects can acts as "transport channels" for anions. At a low voltage bias the electrical current density is not high enough to move ions and to induce electromigration, while an increase of voltage forces oxygen/nitrogen to move to the anode interface along these defects. This process is accompanied by a local rise of temperature which facilitates ion diffusion. The excess of O/N formed at the anode interface (low doped $SrTiO_{3-\delta}$:N layer) is impeding the electron transport (HRS). The electron transport in the HRS and LRS can be described considering the MIS model where a tunnel barrier formation can occur together with inhomogeneous Schottky barrier modifications. Considering both models, a simplified current formula based on the thermomionic emission model is applied and the estimated Schottky barrier height calculated for the HRS is ~0.48 eV, which is in good agreement with theoretically predicted values of ~0.53 eV for the barrier height of $SrTiO_3$/Al junctions. A negligible degradation of the resistive states for more than 10^5 sec suggests good retention properties of the Al/$SrTiO_{3-x}N_y$ memristor. The ratio between high resistance and low resistance states is typically in the range of 10 to 5 and starts to decrease after 10^4 cycles. However, a local heating of the anode interface up to 285 ^{0}C can induce oxidation in air which reduces the lifetime of the memristor. Further studies have to be performed to understand and control the properties of the memristors at various oxygen/nitrogen partial pressures. The model of resistance switching and equivalent circuit representation needs to be validated by further studies on controllable nano-engineering of defects with known concentrations, determination of conduction paths, and on the distribution of local barrier heights during memristor operation.

Acknowledgments

The authors thank V. Raineri, F. La Mattina, I. Riess and L. Gauckler for fruitful remarks and discussions and EMEZ (ETH) for TEM facilities. The work was supported by the Swiss National Science Foundation and by the NCCR MaNEP.

References

[1] Chua L O, 1971 *IEEE Trans. Circuit Theory* **18**(5) 507
[2] Simmons J G and Verderbe R R, 1967 *Proc. R. Soc. London, Ser. A* **301**(1464) 77
[3] Strukov D B, Snider G S, Stewart D R and Williams R S, 2008 *Nat* **453**(7191) 80
[4] Szot K, Speier W, Bihlmayer G and Waser R 2006 *Nat Mater* **5**(4) 312
[5] Tu K N, 2003 *J. Appl. Phys.* **94**(9) 5451
[6] Ho P S and Kwok T 1989 *Rep. Prog. Phys.* **52**(3) 301
[7] Smith R H M, Untiedt C and van Ruitenbeek J M, 2004 *Nanotechnology* **15(7)** S472
[8] Huntington H B and Grone A R, 1961 *J. Phys. Chem. Solids* **20**(1-2) 76
[9] Shkabko A, Aguirre M H, Weidenkaff A, Marozau I and Lippert T, 2009 *Appl. Phys. Lett.* **94**(21) 212102
[10] Schroder D K 2006 *Semiconductor material and device characterization* (Hoboken, N.J.: John Wiley)
[11] Logvinovich D, Borger A, Dobeli M, Ebbinghaus S G, Reller A and Weidenkaff A, 2007 *Prog. Solid State Chem.* **35**(2-4) 281
[12] Verbakel F, Meskers S C J, de Leeuw D M and Janssen R A J 2008 *J. Phys. Chem. C* **112**(14) 5254
[13] Yang J J, Miao F, Pickett M D, Ohlberg D A A, Stewart D R, Lau C N and Williams S R 2009 *Nanotechnology* **20**(21) 215201
[14] Blech I A 1976 *J. Appl. Phys.* **47**(4) 1203
[15] Menke T, Meuffels P, Dittmann R, Szot K and Waser R, 2009 *J. Appl. Phys.* **105**(6) 066104
[16] Shkabko A, Aguirre M H, Marozau I, Dobeli M, Lippert T, Mallepell M andWeidenkaff A 2009 *Mater. Chem. Phys.* **115** 86
[17] Nikawa K 2003 *IEEE Leos Annual Meeting Conference Proceedings, Vols 1 and 2* 742
[18] Sze S M and Ng K K 2007 *Physics of semiconductor devices* (Hoboken, N.J.: Wiley)
[19] Tung R T, 1992 *Phys. Rev. B* **45**(23**)** 13509
[20] Ohdomari I and Tu K N 1980 *J. Appl. Phys.* **51(7)** 3735
[21] Seong D J, Jo M, Lee D and Hwang H 2007 *Electrochem. Solid-State Lett.* **10(**6) H168
[22] Strukov D B and Williams R S, 2009 *Appl. Phys. A.* **94(**3) 515
[23] Shimizu T, Gotoh N, Shinozaki N and Okushi H 1997 *Appl. Surf. Sci.* **117** 400
[24] Robertson J and Chen C W, 1999 *Appl. Phys. Lett.* **74(**8) 1168